Supplementary Material (ESI) for Chemical Communications

Supporting Information

N-type Cascade Electron Transfer along an Oxidative Gradient

Yishi Wu, Yuliang Li, Huixue Li, Qiang Shi, Hongbing Fu,*, and Jiannian Yao*

Beijing National Laboratory for Molecular Science (BNLMS), State Key Laboratory for Structural Chemistry of Unstable and Stable Species, Institute of Chemistry, Chinese Academy of Sciences, Beijing, 100190, P. R. China, [‡] *Beijing National Laboratory for Molecular Sciences (BNLMS), Key Laboratory of Organic Solids, Institute of Chemistry, Chinese Academy of Sciences, Beijing 100190, P. R. China*

Sample Preparation. The ferrocene–perylene tetracarboxylic bisimide (**FcP**) and ferrocene–perylene tetracarboxylic bisimide–fullerene (**FcPF**) were prepared following the same procedures as described previously.[1] The solvents were of chromatographic grade and were used as received.

Quantum Chemical Calculations. The computational calculations were performed by the DFT B3LYP/3-21G(d) method with the GAUSSIAN-03 software package.[2] The graphics of frontier orbitals were generated using the GaussView software.

Picosecond Time-Resolved Fluorescence Measurements. The ps time-resolved fluorescence apparatus has been described as below: The excitation laser pulses (540 nm) were supplied by an optical parametric amplifier (OPA-800CF, Spectra Physics), which was pumped by a regenerative amplifier (Spitfire, Spectra Physics). The excitation energy at the sample was ~100 nJ/pulse. Fluorescence collected with the 90º-geometry was dispersed by a polychromator (250is, Chromex) and detected with a streak camera (C5680, Hamamatsu Photonics). The spectral resolution was 0.2 nm, and the temporal resolution was ~100 ps on the measured delay-time-range setting.

Femtosecond Transient Absorption Spectroscopy. A Ti:sapphire femtosecond laser system provided laser pulses for the femtosecond transient absorption measurements. A regenerative amplifier (Spectra Physics, Spitifire) seeded with a mode-locked Ti:sapphire laser (Spectra Physics, Tsunami) delivered laser pulses at 800 nm (120 fs, 1 kHz), which were then divided into two components by using a 9:1 beam splitter. The major component was sent to an optical parametric amplifier (Spectra Physics, OPA-800CF) to generate the pump pulses (540 nm, 130 fs, 1 kHz). The minor component was further attenuated and focused into a 3-mm sapphire plate to generate the probe pulses. A band-pass filter (SPF-750, CVI) was inserted into the probe beam to select visible probe (450–750 nm) and a long-pass filter (HWB850, Nantong) for near-infrared probe (950–1100 nm). The time delay between the pump and probe beams were regulated through a computer-controlled motorized translation stage in the pump beam. A magic-angle scheme was adopted in the pump-probe measurement. The temporal resolution between the pump and the probe pulses was determined to be ~150 fs (FWHM). The transmitted light was detected by either a liquid-nitrogen cooled CCD (Spectrum One, JY) or an InGaAs linear image sensor (G9203-256D, Hamamatsu) when necessary. The excitation pulsed energy was 0.2 μJ/pulse as measured at the rotating sample cell (optical path length 1 mm). A typical absorbance of

0.4–0.8 at the excitation wavelength was used. The stability of the solutions was spectrophotometrically checked before and after each experiment.

Analysis of the kinetic traces derived from time-resolved spectra was performed individually and globally using nonlinear least-square fitting to a general sum-of-exponentials function after deconvolution of instrument response function (IRF). Decay-associated spectra (DAS) were acquired from global analysis of some representative kinetic traces at selected wavelengths. All the spectroscopic measurements were carried out at room temperature.

(1) Li, Y. J.; Wang, N.; He, X. R.; Wang, S.; Liu, H. B.; Li, Y. L.; Li, X. F.; Zhuang, J. P.; Zhu, D. B. *Tetrahedron* **2005**, *61*, 1563–1569.

(2) Frisch, M. J.; Trucks, G. W.; Schlegel, H. B.; Scuseria, G. E.; Robb, M. A.; Cheeseman, J. R.; Montgomery, J. A., Jr.; Vreven, T.; Kudin, K. N.; Burant, J. C.; Millam, J. M.; Iyengar, S. S.; Tomasi, J.; Barone, V.; Mennucci, B.; Cossi, M.; Scalmani, G.; Rega, N.; Petersson, G. A.; Nakatsuji, H.; Hada, M.; Ehara, M.; Toyota, K.; Fukuda, R.; Hasegawa, J.; Ishida, M.; Nakajima, T.; Honda, Y.; Kitao, O.; Nakai, H.; Klene, M.; Li, X.; Knox, J. E.; Hratchian, H. P.; Cross, J. B.; Bakken, V.; Adamo, C.; Jaramillo, J.; Gomperts, R.; Stratmann, R. E.; Yazyev, O.; Austin, A. J.; Cammi, R.; Pomelli, C.; Ochterski, J. W.; Ayala, P. Y.; Morokuma, K.; Voth, G. A.; Salvador, P.; Dannenberg, J. J.; Zakrzewski, V. G.; Dapprich, S.; Daniels, A. D.; Strain, M. C.; Farkas, O.; Malick, D. K.; Rabuck, A. D.; Raghavachari, K.; Foresman, J. B.; Ortiz, J. V.; Cui, Q.; Baboul, A. G.; Clifford, S.; Cioslowski, J.; Stefanov, B. B.; Liu, G.; Liashenko, A.; Piskorz, P.; Komaromi, I.; Martin, R. L.; Fox, D. J.; Keith, T.; Al-Laham, M. A.; Peng, C. Y.; Nanayakkara, A.; Challacombe, M.; Gill, P. M. W.; Johnson, B.; Chen, W.; Wong, M. W.; Gonzalez, C.; Pople, J. A. Gaussian03, RevisionB.1, Gaussian, Inc., Pittsburgh, PA, 2003.

The equations used for calculating the driving force of electron transfer are listed as follows.[3–4]

$$\Delta G = e[E_{ox}(D) - E_{red}(A)] - \frac{e^2}{4\pi\varepsilon_0\varepsilon_S R_{DA}} - \frac{e^2}{8\pi\varepsilon_0}\left(\frac{1}{r^+} + \frac{1}{r^-}\right)\left(\frac{1}{\varepsilon_{ref}} - \frac{1}{\varepsilon_S}\right) \quad (1)$$

$$\Delta G_{CS} = \Delta G - E_{0-0} \quad (2)$$

$$\Delta G_{CR} = -\Delta G \quad (3)$$

The first oxidation potentials of the donor $E_{ox}(D)$, and the first reduction potentials of the acceptor $E_{red}(A)$ were taken from previous cyclic voltammetry measurements[1] in CH_2Cl_2 (ε_p=9.14). E_{0-0} is the lowest excited singlet state energy of $^1PBI^*$ of **FcPF**, and was determined to be 2.29 eV estimated from the UV-visible absorption spectrum and FL spectrum. The Coulombic terms in present systems are negligible considering the relatively high-polarity dichloromethane used.

(3) Rehm, D.; Weller, A. A. *Isr. J. Chem.* **1970**, *8*, 259–271.

(4) Weller, A. *Z. Phys. Chem. Neue Folge* **1982**, *133*, 93–98.

The equations used for calculating the rate constants of electron transfer and quantum efficiency for charge shift process in **FcPF** are listed as follows:

$$k_{CS} = 1/\tau_{FcP-Abs1} - 1/\tau_{PBI} \quad (4)$$

$$\Phi_{CS} = (1/\tau_{FcP-Abs1} - 1/\tau_{PBI})/1/\tau_{FcPF-Abs1} \quad (5)$$

$$k_{CSh} = 1/\tau_{FcPF-ABS2} - 1/\tau_{FcP-ABS2} \quad (6)$$

$$\Phi_{CSh} = (1/\tau_{FcPF-ABS2} - 1/\tau_{FcP-ABS2})/1/\tau_{FcPF-ABS2} \quad (7)$$

$$k_{CR2} = 1/\tau_{FcPF-ABS3} \quad (8)$$

The values of k_{CS}, k_{CSh}, and k_{CR2} are time constants for charge separation, charge shift, and final charge recombination processes, respectively. The values of Φ_{CS} and Φ_{CSh} are the quantum efficiencies for charge separation and charge shift process, respectively. τ_{PBI} is the measured fluorescence lifetime of the reference compound of *N,N′*-Bis(2-ethylhexane) perylene 3,4,9,10-tetracarboxylic bisimide (**PBI**). $\tau_{FcP-ABS1}$ and $\tau_{FcP-ABS2}$ represent the fast and the long-lived lifetimes derived from global analysis on time-resolved visible absorption spectra of **FcP**. $\tau_{FcPF-ABS1}$ $\tau_{FcP-ABS2}$ and $\tau_{FcPF-ABS3}$ are the fast, the middle and the longest lifetimes from global analysis on time-resolved near-infrared absorption spectra of **FcPF**, respectively.

.

TABLE S1 Apparent decay lifetimes and the relative contribution ratios for **FcP** and **FcPF** in ~10^{-5} mol/L CH_2Cl_2 solutions derived from the kinetic traces of 0→1 transition of PBI's emission at 580 nm.

Compound	Decay lifetime (ns)		χ^2
FcP in CH_2Cl_2	0.24±0.23 (0.51)	4.1±0.1 (0.49)	1.2
FcPF in CH_2Cl_2	0.24±0.12 (0.54)	4.2±0.1 (0.46)	1.1
PBI	–	4.77	–

The contribution ratio of each decay component is given in parentheses.

The value of **PBI** was taken from ref. 5.

(5) Zhang, R. L.; Wang, Z. L.; Wu, Y. S.; Fu, H. B.; Yao, J. N. *Org. Lett.* **2008**, *10*, 3065−3068.

Table S2. Calculated driving forces for charge separation ($-\Delta G_{CS}$) and charge recombination ($-\Delta G_{CR}$) via $^1PBI^*$ and the experimental time constants of charge separation (τ_{CS}), charge shift (τ_{CSh}), and charge recombination (τ_{CR}) of **FcP** and **FcPF** in dichloromethane.

Compound	$-\Delta G_{CS}$ [eV]	$-\Delta G_{CR}$ [eV]	τ_{CS}[a] [ps]	τ_{CR1}[a] [ps]	τ_{CSh}[a] [ps]	τ_{CR2}[a] [ns]
FcP in CH_2Cl_2	1.12	1.17	1.94 ± 0.01	87±1	–	–
FcP in Toluene	<1.12	>1.17	0.51±0.03	970±90	–	–
FcPF in CH_2Cl_2	1.08	1.21	1.94 ± 0.01	87±1	273	1.18±0.02
FcPF in Toluene	<1.08	>1.21	0.59 ± 0.03	1200±100	–	–

[a] Data were obtained from time-resolved absorption studies.

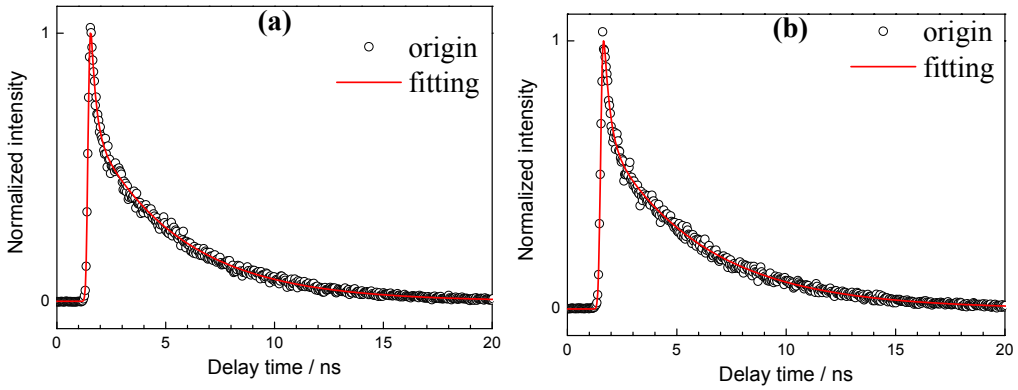

Figure S1. Fluorescence time profiles (black open circles) and corresponding fitting curves (red solid lines) of (a) **FcPF** and (b) **FcP** in dichloromethane solutions (λ_{ex}=540 nm, λ_{probe}=580 nm).

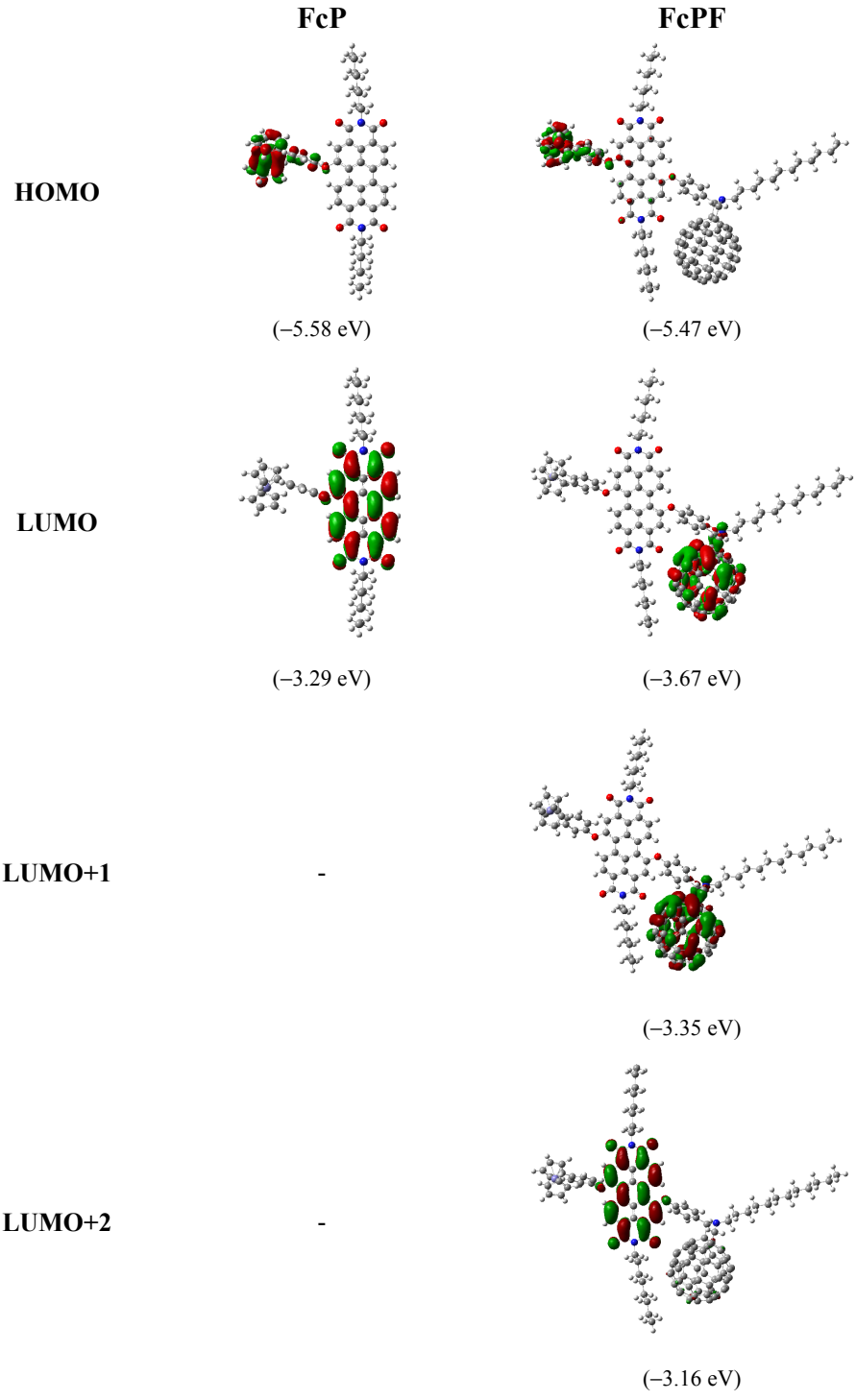

Figure S2. Optimized HOMOs, LUMOs and LUMO+n, together with corresponding energies obtained by DFT methods at the B3LYP/3-21G(d) level for **FcP** and **FcPF**, respectively.

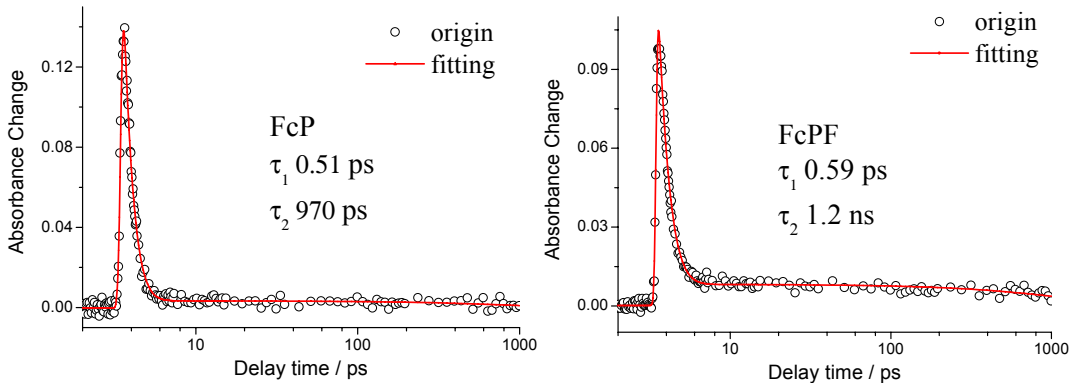

Figure S3. Time-absorption profiles at 720 nm of **FcP** and **FcPF** in toluene solutions. The symbols represent the origin traces and the solid lines represent the fitting curves.